Kuwait J. Sci. Eng. **29**(1) pp. 161 - 180, 2002

An analytical and finite element investigation of all-edge clamped cylindrical panels

ABDULLATEEF M. AL-KHALEEFI*, H.R.H. KABIR* AND SAN-SHYAN LIN**

(*) Department of Civil Engineering, Kuwait University, P.O. Box 5969, 13060 Safat, Kuwait

(**) Department of Harbor & River Engineering, National Taiwan Ocean University Keelung, Taiwan, 20224, ROC

ABSTRACT

A moderately thick all-edge clamped cylindrical panel of isotropic material is investigated using a recently developed closed form approach. The finite element method is employed to calibrate the developed solution. The closed form approach follows a double Fourier series solution method suitable for moderately thick shells. STAAD-III, a commercial package for structural analysis is used to carry out the finite element solution. The through thickness shell formulation of both the approaches is based on the First Order Shear Deformation Theory. The numerical results and comparisons thus presented for various parametric effects should serve as a guideline for engineers.

INTRODUCTION

Since the introduction of shear deformable response into the moderately thick plate by Reissner (1994) and Mindlin (1951) in plate theory, several developments have occurred in shell theory as well, but corresponding progress in the field of boundary-value problems to shells or panels are not abundant in the literature. Analytical solutions to boundary-value problems are very important to check the accuracy of any sort of approximate methods, e.g., finite element, finite difference, Galerkin, or Rayleigh-Ritz, etc. Performances of the finite element method (FEM) in the context of cylindrical panel boundary-value problems are usually compared with a simple type of boundary conditions, such as a simply supported type at all edges (Timoshenko & Woinowsky-Krieger 1959, Flugge 1960, Bert & Kumar 1981, Reddy 1984a,b, Stavky & Lowey 1971). The comparison of the FEM results with the other complex boundary-value-problems was not reported in the literature due to the non-existence of its analytical solutions. Finite element users and developers would like to see the comparison of their solutions with complex boundary-value-problems to have confidence in their models. One knows that the finite element is shy in converging to a solution at edges, an inherent property of the shear-flexible based FEM, in the case of all edge clamped cylindrical panels. The shynesses are due to the element formulation, integration schemes, boundary-value-problems, and number of elements in a solution process. In the aerospace, space-shuttle, or hydrospace industry, shell panels are fabricated in pieces joining them using heavy stringers. When the panels are welded to the heavy stringers, they almost behave as fixed boundary conditions at edges, due to the high inertia ratio of stringers-to-panels. Difficulties lie in the FEM model at those joints. To the best of the knowledge of the authors, the results of the FEM were not compared with the analytical solutions of all edge clamped cylindrical panels, for such analytical solutions were not available in the literature. Kabir and Chaudhuri (1989) have develped an analytical solution to all-edge clamped rectangular plates based on general double Fourier series approach.

The main objective of this paper is to expand this method (Chaudhuri & Kabir 1989) to obtain an analytical solution of a moderately thick all-edge clamped cylindrical panel of isotropic materials subjected to mechanical loadings, such as uniformly distributed loads. The next objective is to compare analytical solutions to validate results obtained from the finite element method.

THEORETICAL BACKGROUND

A cylindrical panel of spans $\ell_1 \times \ell_2$, thickness ℓ_3 and radius r, measured from the mid depth of thickness is shown in Fig. 1. An orthogonal curvilinear co-ordinate system $(\theta_1,\ \theta_2,\ \theta_3)$ is placed at $\frac{\ell_3}{2}$. ℓ_1 and ℓ_2 are measured along θ_1 and θ_2 axes, respectively. The surface generated by $\theta_1 - \theta_2$ is reference surface $(\theta_3 = 0)$. θ_3 is normal to $\theta_1 - \theta_2$ surface. The following are strain - displacement relations according to Sanders' (1959) shell theory for cylindrical panels.

$$\varepsilon_1^0 = \frac{\partial\ u_1^0}{\partial\ \theta_1} + \frac{u_3^0}{r}, \tag{1a}$$

$$\varepsilon_2^0 = \frac{\partial\ u_2^0}{\partial\ \theta_2}, \tag{1b}$$

$$\varepsilon_4^0 = \frac{\partial\ u_3^0}{\partial\ \theta_2} + \phi_2^0, \tag{1c}$$

$$\varepsilon_5^0 = \frac{\partial\ u_3^0}{\partial\ \theta_1} + \phi_1^0 - \frac{u_1^0}{r}, \text{ and} \tag{1d}$$

$$\varepsilon_6^0 = \frac{\partial\ u_1^0}{\partial\ \theta_2} + \frac{\partial\ u_2^0}{\partial\ \theta_1}, \tag{1e}$$

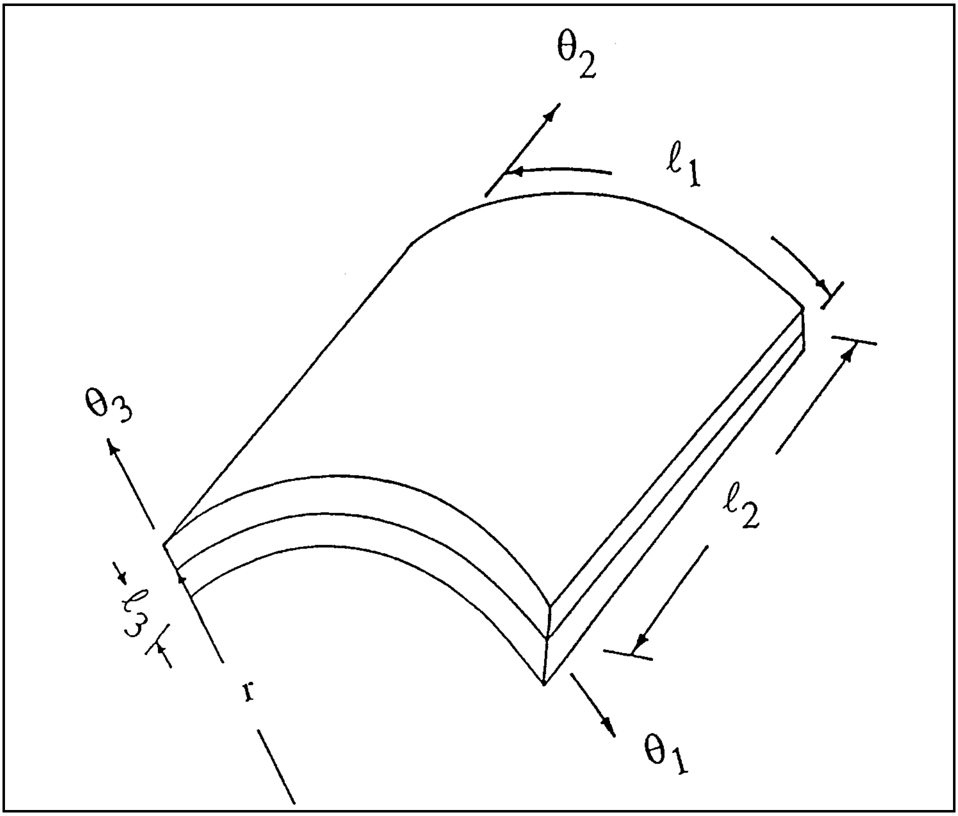

Fig. 1. A cylindrical panel.

where ε_1^0 and ε_2^0 represent surface parallel strain components at $(\theta_1,\ \theta_2,\ \theta_3 = 0)$. ε_4^0 and ε_5^0 are transverse shear strain components in $\theta_1 - \theta_3$ and $\theta_2 - \theta_3$ planes, respectively. ε_6^0 represents the in-plane shear strain. $u_i^0(i = 1 - 3)$ represent displacements of reference surface along $\theta_i(i = 1 - 3)$, respectively.

Following Sanders (1959) the strains at any point along the thickness are expressed in the following form:

$$\varepsilon_1 = \varepsilon_1^0 + \theta_3 \frac{\partial \phi_1}{\partial \theta_1}, \tag{2a}$$

$$\varepsilon_2 = \varepsilon_2^0 + \theta_3 \frac{\partial \phi_2}{\partial \theta_2}, \tag{2b}$$

$$\varepsilon_4 = \varepsilon_4^0, \tag{2c}$$

$$\varepsilon_5 = \varepsilon_5^0, \text{ and} \tag{2d}$$

$$\varepsilon_6 = \varepsilon_6^0 + \theta_3 \left\{ \frac{\partial \phi_2}{\partial \theta_1} + \frac{\partial \phi_1}{\partial \theta_2} - \frac{1}{2}\frac{1}{r}\left(\frac{\partial u_2^0}{\partial \theta_1} - \frac{\partial u_1^0}{\partial \theta_2} \right) \right\} \tag{2e}$$

where ε_i (i = 1, 2, 4, 5, 6) represent strains at $(\theta_1, \theta_2, \theta_3)$. ϕ_1 and ϕ_2 are rotations of normals about θ_2 and θ_1 axes, respectively.

The governing partial differential equations of the cylindrical panel are given as (Chaudhury & Kabir 1989):

$$\frac{\partial N_{11}}{\partial \theta_1} + \frac{\partial N_{66}}{\partial \theta_2} + \frac{1}{2r}\frac{\partial M_{66}}{\partial \theta_2} + \frac{Q_{11}}{r} = 0, \tag{3a}$$

$$\frac{\partial N_{66}}{\partial \theta_1} - \frac{1}{2r}\frac{\partial M_{66}}{\partial \theta_1} + \frac{\partial N_{22}}{\partial \theta_2} = 0, \tag{3b}$$

$$\frac{\partial Q_{11}}{\partial \theta_1} + \frac{\partial Q_{22}}{\partial \theta_2} - \frac{N_{11}}{r} = P_{\theta 3}, \tag{3c}$$

$$\frac{\partial M_{11}}{\partial \theta_1} + \frac{\partial M_{66}}{\partial \theta_2} - Q_{11} = 0, \text{ and} \tag{3d}$$

$$\frac{\partial M_{66}}{\partial \theta_1} + \frac{\partial M_{22}}{\partial \theta_2} - Q_{22} = 0 \tag{3e}$$

where $P\theta_3$ defines uniformly distributed load normal to the surface; N_{ij} define in-plane stress resultants; M_{ij} are stress couple resultants; and Q_{ij} are the transverse shear stress resultants. The stress resultants and stress couple resultants can be expressed in terms of displacements and their derivatives as follows:

$$N_{11} = A\left(\frac{\partial u_1^0}{\partial \theta_1} + \frac{u_3^0}{r} \right) + \upsilon A \frac{\partial u_2^0}{\partial \theta_2}, \tag{4a}$$

$$N_{22} = \upsilon A\left(\frac{\partial u_1^0}{\partial \theta_1} + \frac{u_3^0}{r} \right) + A \frac{\partial u_2^0}{\partial \theta_2}, \tag{4b}$$

$$N_{66} = \frac{1+\upsilon}{2} A\left(\frac{\partial u_1^0}{\partial \theta_2} + \frac{\partial u_2^0}{\partial \theta_1} \right), \tag{4c}$$

$$M_{11} = D\frac{\partial \phi_1}{\partial \theta_1} + \upsilon D \frac{\partial \phi_2}{\partial \theta_2}, \tag{4d}$$

$$M_{22} = \upsilon D\frac{\partial \phi_1}{\partial \theta_1} + D \frac{\partial \phi_2}{\partial \theta_2}, \tag{4e}$$

$$M_{66} = \frac{G\ell_3^3}{12} \left\{ \frac{\partial \phi_1}{\partial \theta_2} + \frac{\partial \phi_2}{\partial \theta_1} - \frac{1}{2r} \left(\frac{\partial u_2^0}{\partial \theta_1} - \frac{\partial u_1^0}{\partial \theta_2} \right) \right\}, \tag{4f}$$

$$Q_{11} = K_1^2 \frac{G\ell_3}{2} + \left(\frac{\partial u_3^0}{\partial \theta_1} + \phi_1 - \frac{u_1^0}{r} \right), \text{ and} \tag{4g}$$

$$Q_{22} = K_2^2 \frac{G\ell_3}{2} + \left(\frac{\partial u_3^0}{\partial \theta_2} + \phi_2 \right) \tag{4h}$$

where

$$A = \frac{E\ell_3}{1+\upsilon^2} \quad ; \quad D = \frac{E\ell_3^2}{12\,(1-\upsilon^2)} \quad \textit{and} \quad G = \frac{E}{2\,(1+\upsilon)} .$$

K_1^1 and K_2^2 are shear correction factors. In our analysis, the values of K_1^1 and K_2^2 are taken as 5/6.

Introduction of equations (4) into (3) produces the following set of partial differential equations:

$$F_{11} u_1 + F_{12} \frac{\partial^2 u_1^0}{\partial \theta_1^2} + F_{13} \frac{\partial^2 u_1^0}{\partial \theta_2^2} + F_{14} \frac{\partial u_2^0}{\partial \theta_1 \partial \theta_2} + F_{15} \frac{\partial u_3^0}{\partial \theta_1} + F_{16} \phi_1$$

$$+ F_{17} \frac{\partial^2 \phi_1}{\partial \theta_2^2} + F_{18} \frac{\partial^2 \phi_1}{\partial \theta_1 \partial \theta_2} = 0 \tag{5a}$$

$$F_{21} \frac{\partial u_1^0}{\partial \theta_1 \partial \theta_2} + F_{23} \frac{\partial^2 u_2^0}{\partial^2 \theta_2} + F_{24} \frac{\partial^2 u_2}{\partial \theta_2^2} + F_{25} \frac{\partial u_3}{\partial \theta_2} + F_{26} \phi_2$$

$$+ F_{27} \frac{\partial^2 \phi_2}{\partial^2 \theta_1} + F_{28} \frac{\partial^2 \phi_1}{\partial \theta_1 \partial \theta_2} = 0 , \tag{5b}$$

$$F_{31} \frac{\partial u_1^0}{\partial \theta_1} + F_{32} \frac{\partial u_2^0}{\partial \theta_2} + F_{33} u_3^0 + F_{34} \frac{\partial^2 u_3^0}{\partial \theta_1^2} + F_{35} \frac{\partial^2 u_3^0}{\partial \theta_2^2}$$

$$+ F_{36} \frac{\partial \phi_1}{\partial \theta_1} + F_{37} \frac{\partial \phi_2}{\partial \theta_2} = q , \tag{5c}$$

$$F_{41} u_1^0 + F_{42} \frac{\partial^2 u_1^0}{\partial \theta_2^2} + F_{43} \frac{\partial u_2^0}{\partial \theta_1 \partial \theta_2} + F_{44} \frac{\partial u_3^0}{\partial \theta_1} + F_{45} \phi_1 + F_{46} \frac{\partial^2 \phi_1}{\partial^2 \theta_1}$$

$$+ F_{47} \frac{\partial^2 \phi_1}{\partial^2 \theta_2} + F_{48} \frac{\partial \phi_2}{\partial \theta_1 \partial \theta_2} = 0 , \text{ and} \tag{5d}$$

$$F_{51} \frac{\partial^2 u_1^0}{\partial \theta_1 \partial \theta_2} + F_{52} \frac{\partial^2 u_2^0}{\partial^2 \theta_1} + F_{53} \frac{\partial u_3^0}{\partial \theta_2} + F_{54} \frac{\partial^2 \phi_1}{\partial \theta_1 \partial \theta_2}$$

$$+ F_{55} \phi_2 + F_{56} \frac{\partial^2 \phi_2}{\partial^2 \theta_2} = 0 \tag{5e}$$

where F_{ij} are as defined in the Appendix.

The natural boundary conditions for all edge clamped cylindrical panels are:

$$u_1^0 = 0 \quad \text{at all edges , and} \tag{6a}$$

$$\phi_i = 0 \quad \text{at all edges.} \tag{6b}$$

EXACT SOLUTION

The objective here is to obtain an exact solution of the partial differential equations (5a through 5e) for the prescribed boundary conditions as given in equations (6a and 6b). The displacements functions are assumed in terms of double Fourier series in the following form (Kabir & Chaudhury 1994):

$$u_i^0 = \sum_{m=1}^{\infty} \sum_{n=1}^{\infty} \left\{ A_{mn}^i \sin(\alpha_m \theta_1) \sin(\beta_n \theta_2) \right\} \quad i = 1, 2, 3 \text{ , and} \tag{7a}$$

$$\phi_i = \sum_{m=1}^{\infty} \sum_{n=1}^{\infty} \left\{ B_{mn}^i \sin(\alpha_m \theta_1) \sin(\beta_n \theta_2) \right\} \quad i = 1, 2 \tag{7b}$$

where A^i_{mm} and B^i_{mm} are Fourier constants. α_m and β_m are defined as $\frac{m\pi}{\ell_1}$ and $\frac{n\pi}{\ell_1}$, respectively. The above assumed solution functions satisfy the prescribed boundary conditions in a manner similar to Navier's approach (cited in Timoshenko & Woinowsky-Krieger 1959). Therefore, their further differentiation would not pose any violation of the physical continuity. Expansion of the transverse load into double Fourier series:

$$P_{\theta 3} = \sum_{m=1}^{\infty} \sum_{n=1}^{\infty} q_{mn} \sin(\alpha_m \theta_1) \sin(\beta_n \theta_2) \tag{8}$$

followed by introduction of the assumed solution functions (7) and their corresponding derivatives into the governing partial differential equations (5), generates the following sets of linear algebraic equations:

$$\begin{Bmatrix} F_1^1 \\ F_4^1 \end{Bmatrix}^T \begin{Bmatrix} A_{mn}^1 \\ B_{mn}^1 \end{Bmatrix} \sin(\alpha_m \theta_1) \sin(\beta_n \theta_2)$$

$$+ \begin{Bmatrix} F_2^1 \\ F_5^1 \end{Bmatrix}^T \begin{Bmatrix} A_{mn}^2 \\ B_{mn}^2 \end{Bmatrix} \cos(\alpha_m \theta_1) \cos(\beta_n \theta_2)$$

$$+ \ F_3^1 \ A_{mn}^3 \ \cos\left(\alpha_m \ \theta_1\right) \ \sin\left(\beta_n \ \theta_2\right) = 0$$

for m = 1, ..., ∞ and n = 1, ..., ∞ , (9a)

$$\begin{Bmatrix} F_2^2 \\ F_5^2 \end{Bmatrix}^T \begin{Bmatrix} A_{mn}^2 \\ B_{mn}^2 \end{Bmatrix} \sin\left(\alpha_m \ \theta_1\right) \ \sin\left(\beta_n \ \theta_2\right)$$

$$+ \begin{Bmatrix} F_1^2 \\ F_4^2 \end{Bmatrix}^T \begin{Bmatrix} A_{mn}^1 \\ B_{mn}^1 \end{Bmatrix} \cos\left(\alpha_m \ \theta_1\right) \ \cos\left(\beta_n \ \theta_2\right)$$

$$+ \ F_3^2 \ A_{mn}^3 \ \sin\left(\alpha_m \ \theta_1\right) \cos\left(\beta_n \ \theta_2\right) = 0$$

for m = 1, ..., ∞ and n = 1, ..., ∞ , (9b)

$$\left\{F_3^3\right\}\left\{A_{mn}^3\right\} \sin\left(\alpha_m \ \theta_1\right) \sin\left(\beta_n \ \theta_2\right)$$

$$+ \begin{Bmatrix} F_2^3 \\ F_5^3 \end{Bmatrix}^T \begin{Bmatrix} A_{mn}^2 \\ B_{mn}^2 \end{Bmatrix} \sin\left(\alpha_m \ \theta_1\right) \cos\left(\beta_n \ \theta_2\right)$$

$$+ \begin{Bmatrix} F_1^3 \\ F_4^3 \end{Bmatrix}^T \begin{Bmatrix} A_{mn}^1 \\ B_{mn}^1 \end{Bmatrix} \cos\left(\alpha_m \ \theta_1\right) \sin\left(\beta_n \ \theta_2\right)$$

$$= \ q_{mn} \ \sin\left(\alpha_m \ \theta_1\right) \sin\left(\beta_n \ \theta_2\right)$$

for m = 1, ..., ∞ and n = 1, ..., ∞ , (9c)

$$\begin{Bmatrix} F_1^4 \\ F_4^4 \end{Bmatrix}^T \begin{Bmatrix} A_{mn}^1 \\ B_{mn}^1 \end{Bmatrix} \sin\left(\alpha_m \ \theta_1\right) \sin\left(\beta_n \ \theta_2\right)$$

$$+ \begin{Bmatrix} F_2^4 \\ F_5^4 \end{Bmatrix}^T \begin{Bmatrix} A_{mn}^2 \\ B_{mn}^2 \end{Bmatrix} \cos\left(\alpha_m \ \theta_1\right) \cos\left(\beta_n \ \theta_2\right)$$

$$+ \ F_3^4 \ A_{mn}^3 \ \cos\left(\alpha_m \ \theta_1\right) \sin\left(\beta_n \ \theta_2\right) = 0$$

for m = 1, ..., ∞ and n = 1, ..., ∞ , (9d)

$$\begin{Bmatrix} F_2^5 \\ F_5^5 \end{Bmatrix}^T \begin{Bmatrix} A_{mn}^2 \\ B_{mn}^2 \end{Bmatrix} \sin\left(\alpha_m \ \theta_1\right) \sin\left(\beta_m \ \theta_2\right)$$

$$+ \begin{Bmatrix} F_1^5 \\ F_4^5 \end{Bmatrix} \begin{Bmatrix} A_{mn}^1 \\ B_{mn}^1 \end{Bmatrix} \cos\left(\alpha_m \ \theta_1\right) \cos\left(\beta_m \ \theta_2\right)$$

$$+ \left\{F_3^5\right\}\left\{A_{mn}^3\right\} \ \sin\left(\alpha_m \ \theta_1\right) \cos\left(\beta_n \ \theta_2\right) = 0$$

for m = 1, ..., ∞ and n = 1, ..., ∞ (9e)

where F_j^i (i = 1,5; j = 1, 5) are constant coefficients.

Equations (9a - 9e) yield a total of 15 mn (for m = 1, ... ∞, and n = 1,... ∞) algebraic equations can be generated, if a direct application of Navier's type is employed, in 5mn unknowns $\left(u_1^0, u_2^0, u_3^0, \phi_1, \phi_2\right)$, thus failing to provide a unique solution to this physical problem. Now the following series expansions of cos (α_m θ_1) cos (β_n θ_2), cos (α_m θ_1) sin (β_n θ_2), and sin (α_m θ_1) cos (β_n θ_2) are performed (Sanders 1959, Chaudhuri & Kabir 1989, Kabir 1994):

$$\cos\left(\alpha_m\,\theta_1\right)\cos\left(\beta_n\,\theta_2\right) = \sum_m^\infty \sum_n^\infty f_{\overline{m}m}\; g_{\overline{n}n}\,\sin\left(\gamma_{\overline{m}}\,\theta_1\right)\sin\left(\psi_{\overline{n}}\,\theta_2\right), \tag{10a}$$

$$\cos\left(\alpha_m\,\theta_1\right)\sin\left(\beta_n\,\theta_2\right) = \sum_m^\infty f_{\overline{m}m}\,\sin\left(\gamma_{\overline{m}}\,\theta_1\right)\sin\left(\beta_n\,\theta_2\right), \text{ and} \tag{10b}$$

$$\sin\left(\alpha_m\,\theta_1\right)\cos\left(\beta_n\,\theta_2\right) = \sum_n^\infty g_{\overline{n}n}\,\sin\left(\alpha_m\,\theta_1\right)\sin\left(\psi_{\overline{n}}\,\theta_2\right), \tag{10c}$$

where

$$f_{\overline{m}m} = \frac{4}{m\,\pi\left(1-\dfrac{\overline{m}^2}{m^2}\right)}, \tag{11a}$$

$$\frac{\overline{m}}{m} \neq 1 \qquad \overline{m} = 1, 2, 3, ..., \infty \tag{11b}$$

$$g_{\overline{n}n} = \frac{4}{n\,\pi\left(1-\dfrac{\overline{n}^2}{n^2}\right)}, \tag{12a}$$

$$\frac{\overline{n}}{n} \neq 1 \qquad \overline{n} = 1, 2, 3, ..., \infty, \tag{12b}$$

$$\gamma_{\overline{m}} = \frac{\pi\overline{m}}{\ell_1}, \text{ and} \tag{13a}$$

$$\psi_{\overline{n}} = \frac{\pi\overline{n}}{\ell_2}. \tag{13b}$$

Introduction of the above series expansions (11 - 13) into equation (9a - 9e) will now provide as many equations in as many unknowns, thus providing a unique solution to an important boundary value problem. The solution of the simultaneous equations would provide the displacement terms: u_1, u_2, u_3, ϕ_1 and ϕ_2, as assumed in the solution functions (7).

NUMERICAL RESULTS AND DISCUSSIONS

To demonstrate the above procedure numerically, a cylindrical panel subjected to uniformly distributed load with the following material properties is considered.

$E = 29{,}000$ ksi (204 GPa) ,

$\upsilon = 0.25$,

$K_1^2 = 5/6$ (for a rectangular cross-section) , and

K_1^2 : transverse shear correction factor.

For convenience the following non dimensionalized quantities are defined:

$$u_3^* = \frac{1000\, E\ell_3^3\, u_3}{P_{\theta 3}\, \ell_1^2} ,$$

$$M_1^* = \frac{1000\, M_1}{P_{\theta 3}\, \ell_1^2} , \text{ and}$$

$$M_2^* = \frac{1000\, M_2}{P_{\theta 3}\, \ell_1^2} .$$

The accuracy of a series solution lies to the nature of convergency. A monotonic convergence of a double Fourier series in the sense of Navier's solution is well achieved (Timoshenko & Woinowsky-Krieger 1959, Flugge 1960) as it satisfies the boundary conditions and governing differential

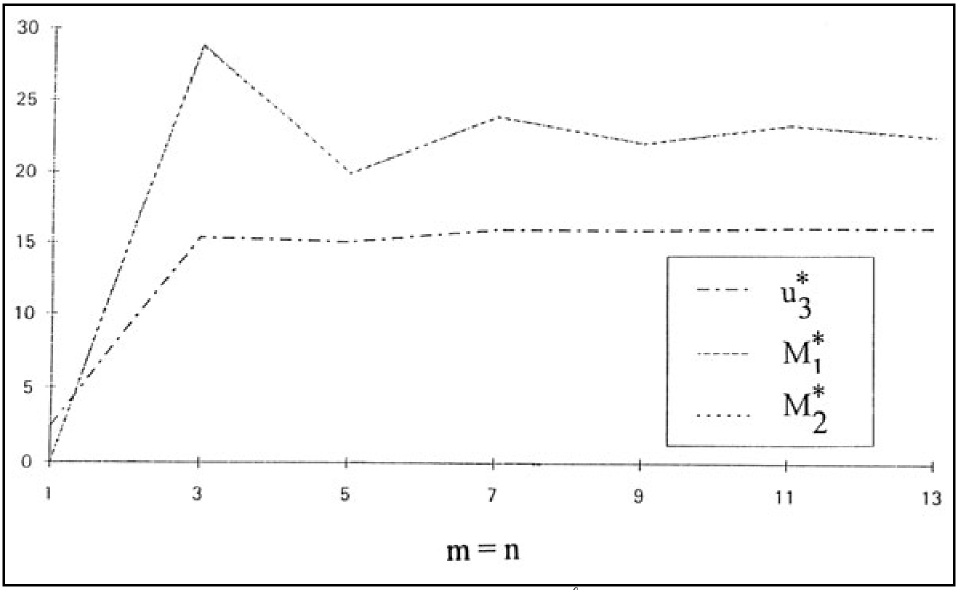

Fig. 2. Convergence of u_3^* , M_1^* and M_2^* with $m = n$, $\frac{\ell_2}{\ell_1} = 1$, $\ell_1/\ell_3 = 10$ and $r/\ell_1 = 10$.

equations. However, in the present case a series expansion into a series solution is introduced, which is a distinct deviation from Navier's approach. Therefore, study of the nature of convergency for the present situation will be a very interesting one.

Figs. 2 and 3 illustrate the convergences of u_3^* , M_1^* and M_2^* (central values) for

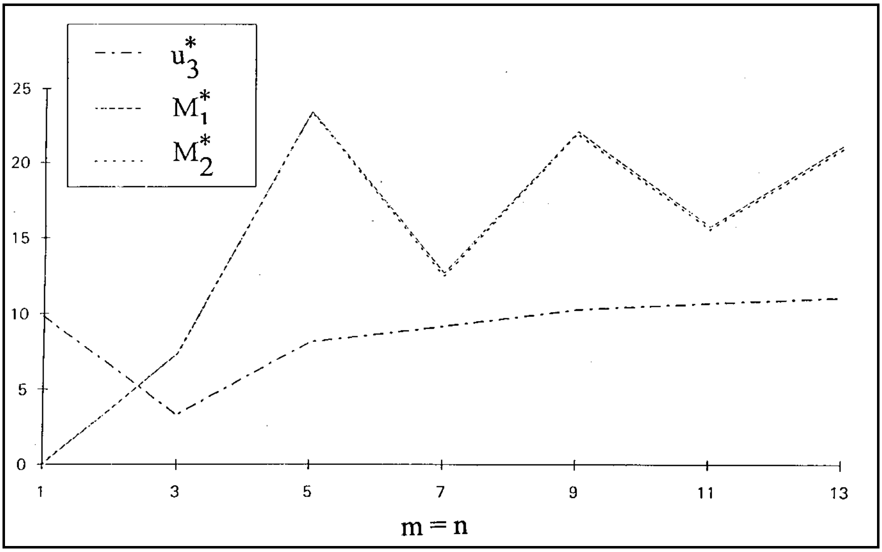

Fig. 3. Convergence of u_3^* , M_1^* and M_2^* with $m = n$, $\frac{\ell_2}{\ell_1} = 1$, $\ell_1/\ell_3 = 50$ and $r/\ell_1 = 10$.

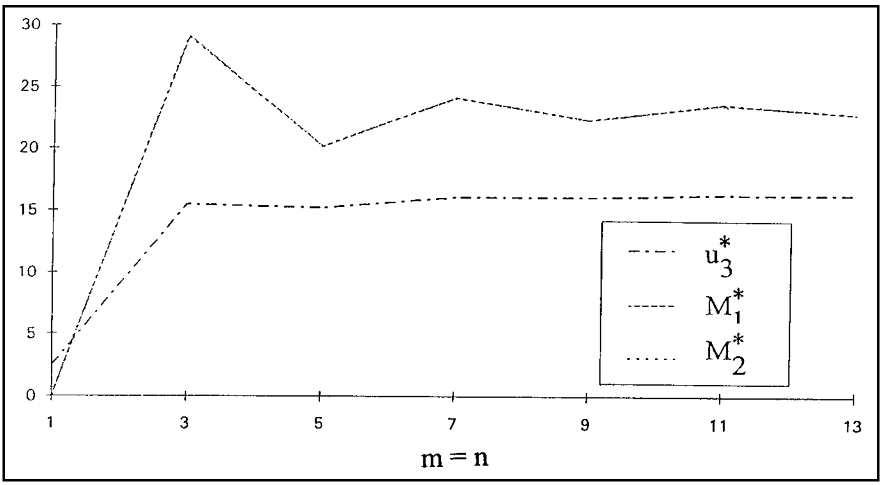

Fig. 4. Convergence of u_3^* , M_1^* and M_2^* with $m = n$, $\frac{\ell_2}{\ell_1} = 1$, $\ell_1/\ell_3 = 10$ and $r/\ell_1 = 1000$.

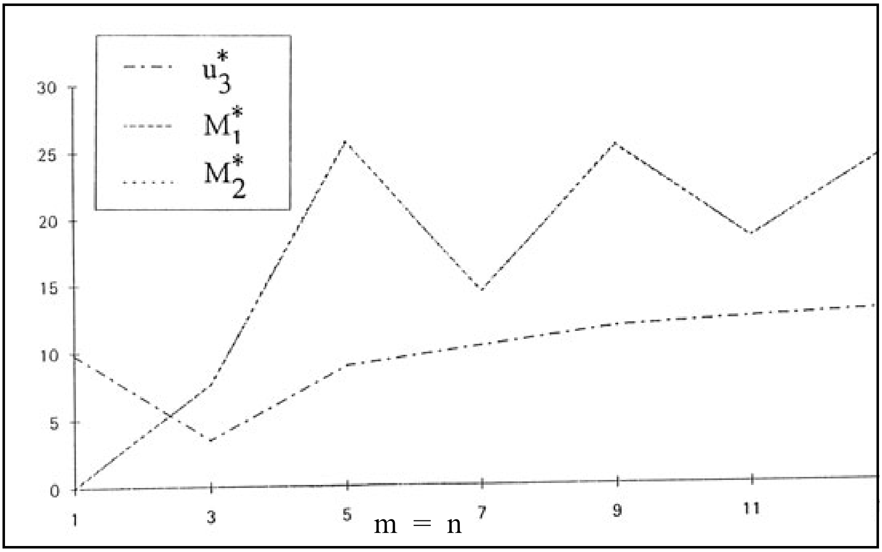

Fig. 5. Convergence of u_3^* , M_1^* and M_2^* with $m = n$, $\frac{\ell_2}{\ell_1} = 1$, $\ell_1/\ell_3 = 50$ and $r/\ell_1 = 1000$.

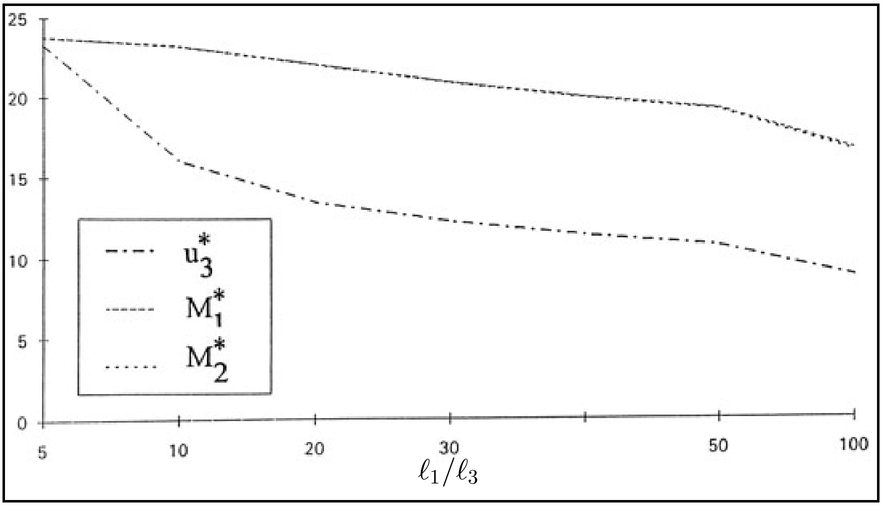

Fig. 6. Variations of u_3^* , M_1^* and M_2^* with $\frac{\ell_2}{\ell_1} = 1$, and $r/\ell_1 = 20$ for various ℓ_1/ℓ_3.

various m = n with $\ell_2/\ell_1 = 1$, $r/\ell_1 = 10$, and $\ell_2/\ell_1 = 1$, $r/\ell_1 = 10$ and 50, respectively. A monotonic convergence for the case of $\ell_1/\ell_3 = 10$ is well achieved, while $\ell_1/\ell_3 = 50$ shows monotonic oscillations but converges to the average values, a nature of double Fourier series expansion. Figures 4 and 5 illustrate the convergence of u_3^* , M_1^* and M_2^* for various m = n with $\ell_2/\ell_1 = 1$, and $r\ell_1 = 1000$ and $\ell_1/\ell_3 = 10$ and 50, respectively, and similar trends are also observed here.

Variations of u_3^* , M_1^* and M_2^* (central values) for various ℓ_1/ℓ_3 are given for a cylindrical panel with $\ell_2/\ell_1 = 1$, r/ℓ_1 , 20, 30, 40, 50, 100 and 500, respectively, in Figs. 6 to 11. The characteristics and trends of the results are very convincing. The parametric variations with respect to various radius-to-span ratios are given for u_3^*, M_1^* and M_2^* (central values) in Figs. 12 to 16. The effects of radius for the present problem are not appreciable.

The numerical results of the present solution are compared with a commercially available structural analysis package, STAAD - III (1998). The panel is modeled

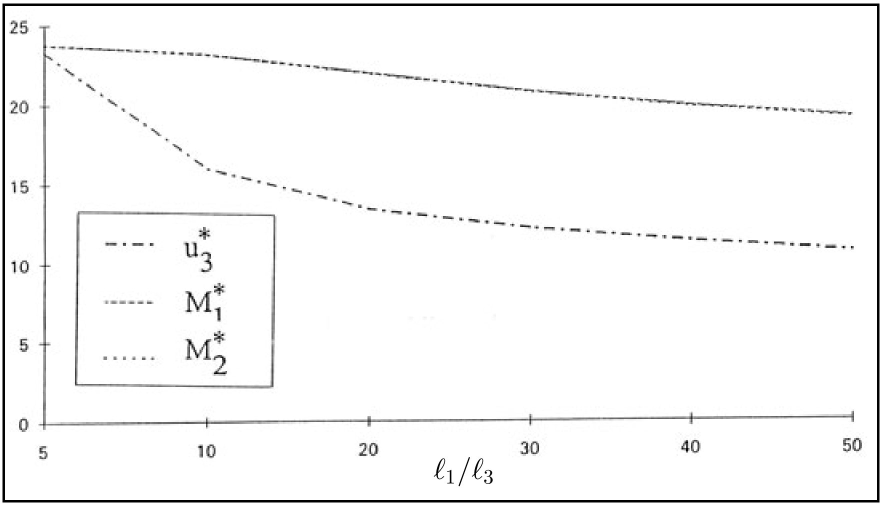

Fig. 7. Variations of u_3^* , M_1^* and M_2^* with $\frac{\ell_2}{\ell_1} = 1$, and $r/\ell_1 = 30$ for various ℓ_1/ℓ_3.

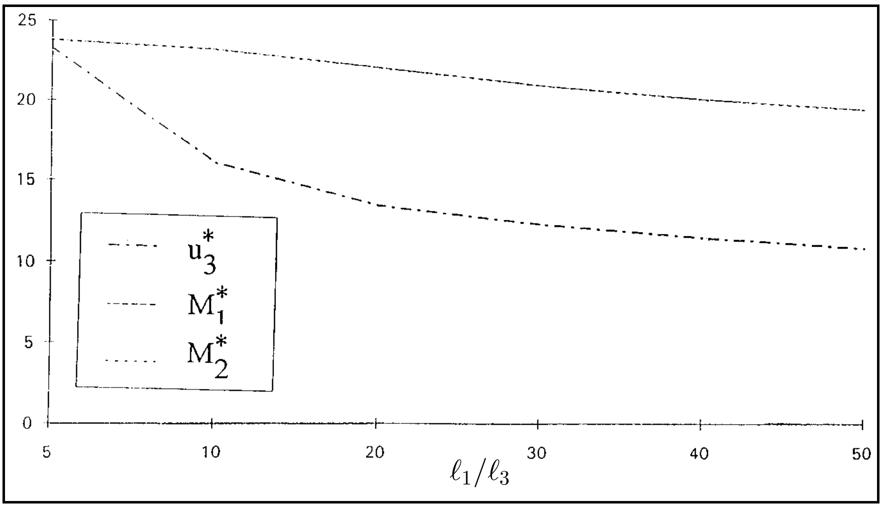

Fig. 8. Variations of u_3^* , M_1^* and M_2^* with $\frac{\ell_2}{\ell_1} = 1$, and $r/\ell_1 = 40$ for various ℓ_1/ℓ_3.

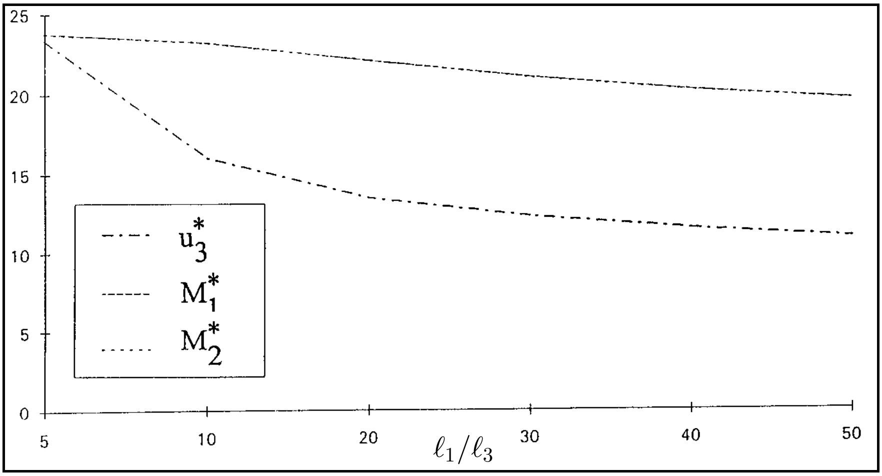

Fig. 9. Variations of u_3^* , M_1^* and M_2^* with $\frac{\ell_2}{\ell_1} = 1$, and $r/\ell_1 = 50$ for various ℓ_1/ℓ_3.

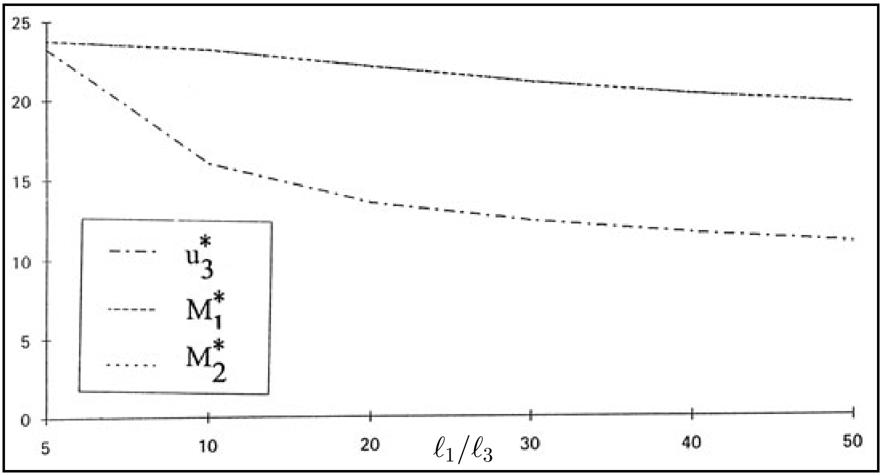

Fig. 10. Variations of u_3^* , M_1^* and M_2^* with $\frac{\ell_2}{\ell_1} = 1$, and $r/\ell_1 = 100$ for various ℓ_1/ℓ_3.

with $N \times N$ where N is the number of elements, ($N = 5$ to 27) 4 - node quadrilateral plate element. It is a hybrid element with complete quadratic stress distribution. The assumed stress distribution is as follows (STAAD-III, 1998):

$$\begin{pmatrix} \sigma_x \\ \sigma_y \\ \tau_{xy} \end{pmatrix} = \begin{bmatrix} 1 & x & y & 0 & 0 & 0 & 0 & x^2 & 2xy & y^2 & 0 & 0 \\ 0 & 0 & 0 & 1 & x & y & 0 & y^2 & 0 & 0 & x^2 & 2xy \\ 0 & -y & 0 & 0 & 0 & -x & 1 & -2xy & -y^2 & 0 & 0 & -x^2 \end{bmatrix} \begin{pmatrix} a_1 \\ a_2 \\ a_3 \\ \cdot \\ \cdot \\ a_{12} \end{pmatrix} \quad (14)$$

a_1 through a_{12} are constants of stress polynomials.

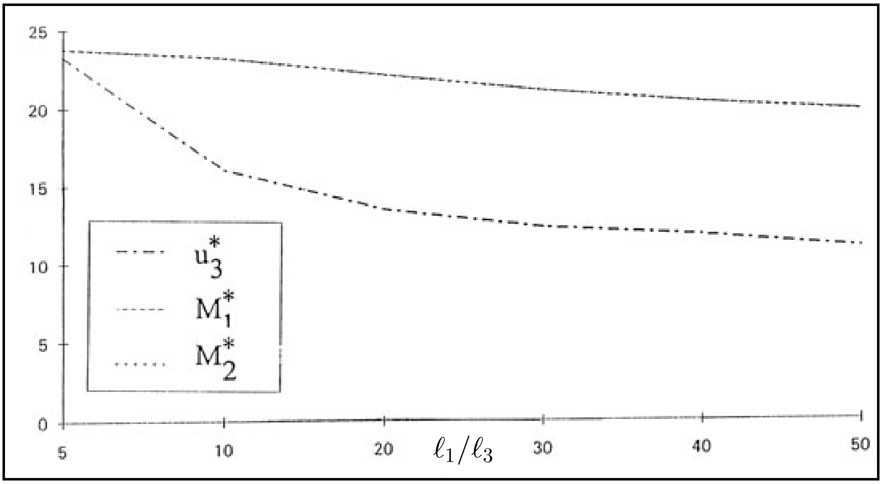

Fig. 11. Variations of u_3^* , M_1^* and M_2^* with $\frac{\ell_2}{\ell_1} = 1$, and $r/\ell_1 = 500$ for various ℓ_1/ℓ_3.

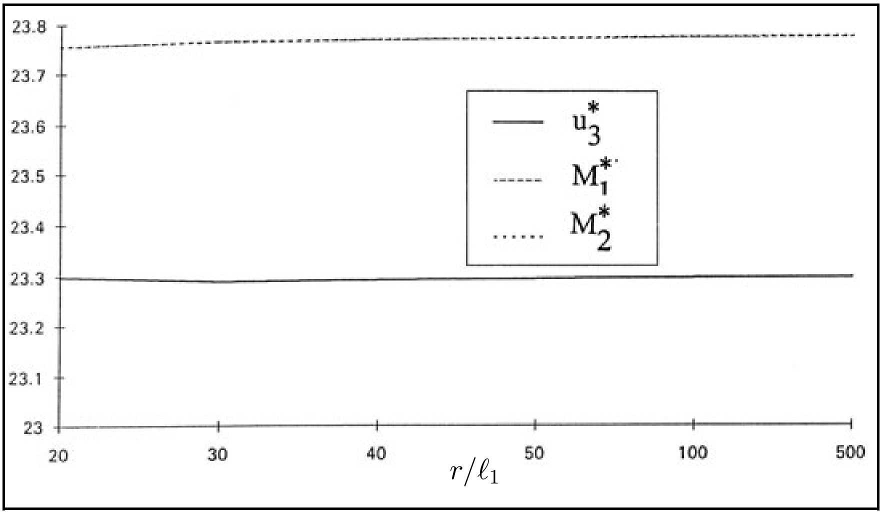

Fig. 12. Variations of u_3^* , M_1^* and M_2^* with $\frac{\ell_2}{\ell_1} = 1$, and $\ell_1/\ell_3 = 5$ for various r/ℓ_1.

The results of u_3^* , M_1^* and M_2^* (centrally calculated) are plotted in Fig. 17 along with the present solutions (with m = n = 9). An oscillation is observed for finite element results for the case of stress resultant, while transverse displacements agree very much with the present solution. The oscillation can be attributed to the condition that finite element solutions, depending on the complexity of boundary conditions, may show oscillation.

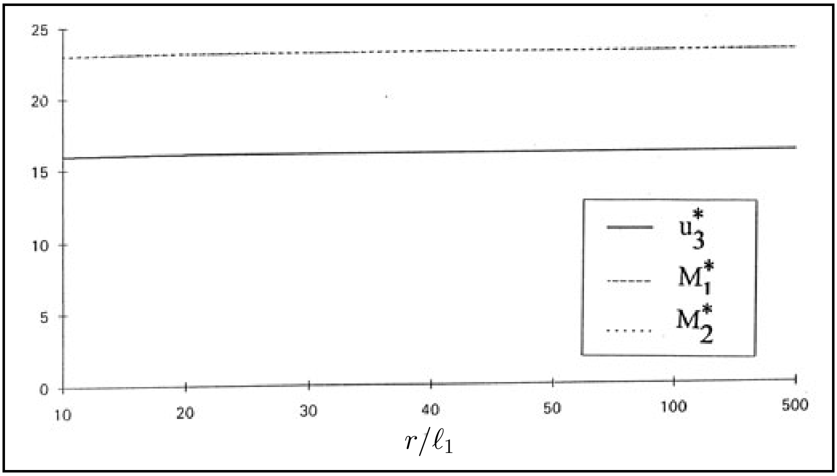

Fig. 13. Variations of u_3^* , M_1^* and M_2^* with $\frac{\ell_2}{\ell_1} = 1$, and $\ell_1/\ell_3 = 10$ for various r/ℓ_1.

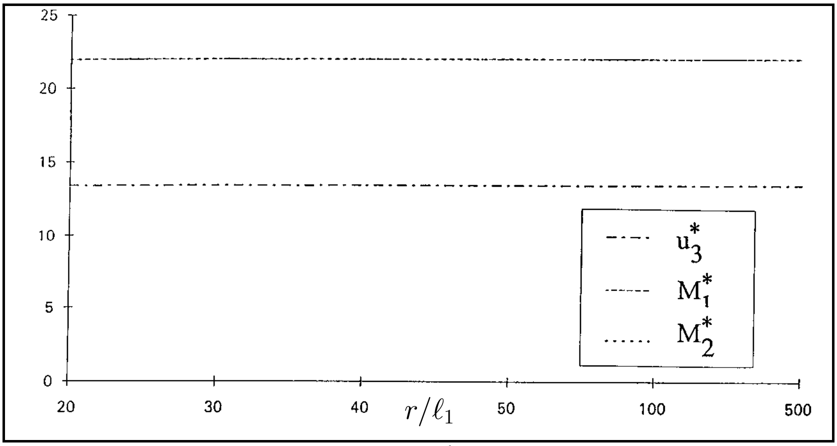

Fig. 14. Variations of u_3^* , M_1^* and M_2^* with $\frac{\ell_2}{\ell_1} = 1$, and $\ell_1/\ell_3 = 20$ for various r/ℓ_1.

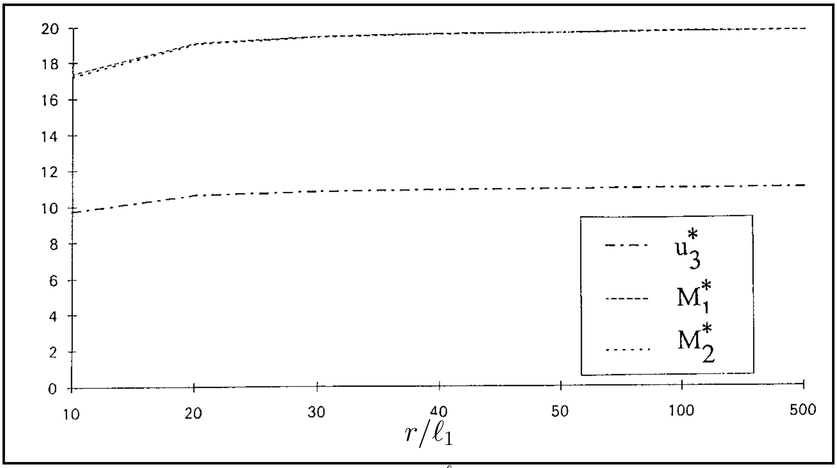

Fig. 15. Variations of u_3^* , M_1^* and M_2^* with $\frac{\ell_2}{\ell_1} = 1$, and $\ell_1/\ell_3 = 50$ for various r/ℓ_1.

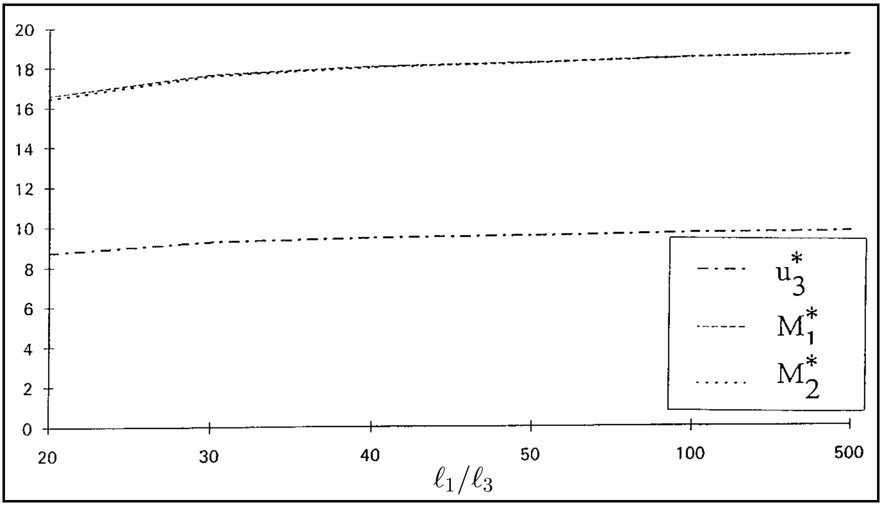

Fig. 16. Variations of u_3^*, M_1^* and M_2^* with $\frac{\ell_2}{\ell_1} = 1$, and $\ell_1/\ell_3 = 100$ for various r/ℓ_1.

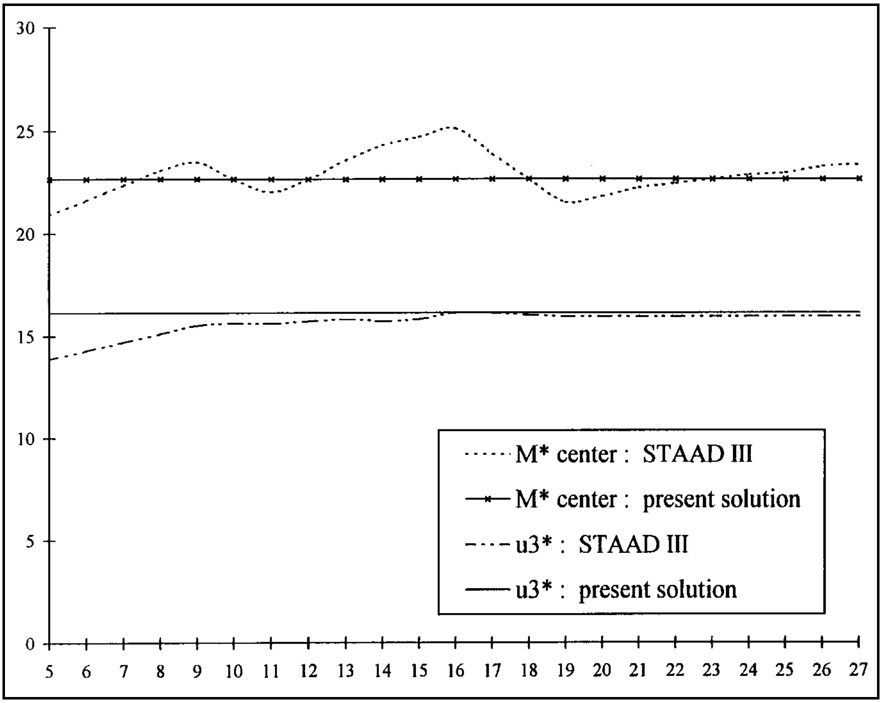

Fig. 17. Comparison of present and STAAD-III solutions for u_3^*, and M_1^* (central values) of cylindrical panel with $\frac{\ell_1}{\ell_3} = 20, \frac{\ell_2}{\ell_1} = 1$, and $\frac{r}{\ell_1} = 10$.

CONCLUSION

An analytical solution to a clamped cylindrical panel is presented. The shell formulation, based on Sanders' kinematic relation generates five coupled partial differential equations that are solved using the recently developed double Fourier series approach. The accuracy of the series solution is determined numerically. The numerical results of the present solution are compared with the numerical results of STAAD-III. The numerical results thus presented can be used as base-line solutions to compare other approximate methodologies. The extension of the method as presented here is under consideration for thermal and in-plane shear buckling problems.

ACKNOWLEDGEMENTS

The authors wish to thank Engr. Muzibul Haque and Engr. Shamsul Haque for their help in plotting figures. Special thanks to Mrs. Mini Kora for carefully typing the manuscript.

REFERENCES

Bert, C.W. & Kumar, M. 1981. Vibration of cylindrical shells of bi-modulus composite materials. Journal of Sound and Vibration **81**: 107-121.

Chaudhury, R. A. and Kabir, H. R. H. 1989. "On analytical solutions to BVPs of doubly-curved moderately-thick orthotropic shells. International Journal of Engineering Science., **27 (11)**: 1325-1336.

Flugge, W. 1960. Stresses in shells. 2nd Edition, Julius Springer, Berlin, Germany.

Green, A.E. 1944. Double Fourier series and boundary value problems. Proceedings of Cambridge Philosophical Society **40**: 222-228.

Kabir, H.R.H. & Chaudhury, R. A. 1994. On Gibbs - Phenomenon - free Fourier Solution for finite shear - flexible laminated clamped curved panels. International Journal of Engineering Science **15 (3):** 501-520.

Kabir, H.R.H. 1994. Static responses of anti-symmetric angle-ply laminated shear-flexible clamped plates. Computers and Structures **53**: 201-208.

Mindlin, R.D. 1951. Influence of rotatory inertia and shear on flexural motion of isotropic elastic plates. Journal of Applied Mechanics **18**: 31-38.

Reddy, J.N. 1984a. Energy and variational methods in applied mechanics. John Wiley & Sons, New York, NY, USA.

Reddy, J.N. 1984b. Exact solutions of moderately-thick laminated shells. Journal of Engineering Mechanics ASCE **110**: 794-809.

Reissner, E. 1994. On the theory of bending of elastic plates. Journal of Mathematical Physics **23**: 184-191.

Sanders, J.L. Jr. 1959. An improved first-approximation theory for thin shells. NASA Technical Report R-24.

STAAD-III, 1998. Version 22.3, Research Engineers Inc., Yorba Linda, CA, USA.

Stavsky, Y. & Lowey, R. 1971. On vibration of heterogeneous orthotropic cylindrical shells. Journal of Sound and Vibration **15**: 235-256.

Timoshenko, S.P. & Woinowsky-Krieger, S. 1959. Theory of plates and shells. 2nd Edition, McGraw-Hill., New York, NY, USA.

(Submtted 13 February 2000)
(Revised 16 April 2001)
(Accepted 25 April 2001)

APPENDIX

Definitions of coefficients as defined in equations (5a - 5e):

$$F_{11} = -K_1^2 \frac{G\ell_3}{2r^2}$$

$$F_{12} = A$$

$$F_{13} = \frac{1+\upsilon}{2} A + \frac{1}{4r^2} \frac{G\ell_3^3}{12}$$

$$F_{14} = \upsilon A + \frac{1+\upsilon}{2} A - \frac{1}{4r^2} \frac{G\ell_3^3}{12}$$

$$F_{15} = \frac{A}{r} + K_1^2 \frac{G\ell_3}{2r}$$

$$F_{16} = K_1^2 \frac{G\ell_3}{2r}$$

$$F_{17} = \frac{1}{2r} \frac{G\ell_3^3}{12}$$

$$F_{18} = \frac{1}{2r} \frac{G\ell_3^3}{12}$$

$$F_{21} = \frac{1+\upsilon}{2} A - \frac{1}{4r^2} \frac{G\ell_3^3}{12} + \upsilon A$$

$$F_{23} = \frac{1+\upsilon}{2} A + \frac{1}{4r^2} \frac{G\ell_3^2}{12}$$

$$F_{24} = A$$

$$F_{25} = \frac{\upsilon}{r} A$$

$$F_{27} = -\frac{1}{2r} \frac{G\ell_3^3}{12}$$

$$F_{28} = -\frac{1}{2r} \frac{G\ell_3^3}{12}$$

$$F_{31} = -K_1^2 \frac{G\ell_3}{2r} - \frac{\upsilon}{r} A - \frac{1}{r} A$$

$$F_{32} = -\frac{\upsilon}{r}A$$

$$F_{33} = -\frac{1}{r^2}A$$

$$F_{34} = K_1^2\frac{G\ell_3}{2}$$

$$F_{35} = K_1^2\frac{G\ell_3}{2}$$

$$F_{36} = K_1^2\frac{G\ell_3}{2}$$

$$F_{37} = K_1^2\frac{G\ell_3}{2}$$

$$F_{41} = K_1^2\frac{G\ell_3}{2r}$$

$$F_{42} = \frac{1}{2r}\frac{G\ell_3^3}{12}$$

$$F_{43} = -\frac{1}{2r}\frac{G\ell_3^3}{12}$$

$$F_{44} = -K_1^2\frac{G\ell_3}{2}$$

$$F_{45} = -K_1^2\frac{G\ell_3}{2}$$

$$F_{46} = D$$

$$F_{47} = \frac{G\ell_3^3}{12}$$

$$F_{48} = \upsilon D\frac{G\ell_3^3}{12}$$

$$F_{51} = \frac{1}{2r}\frac{G\ell_3^3}{12}$$

$$F_{52} = -\frac{1}{2r}\frac{G\ell_3^3}{12}$$

$$F_{53} = -K_1^2\frac{G\ell_3}{2}$$

$$F_{54} = \frac{G\ell_3^3}{12} + \upsilon D$$

$$F_{55} = -K_1^2\frac{G\ell_3}{2}$$

$$F_{56} = D$$

تحريات تحليلية وعناصر محدودة للصفيحة الأسطوانية ذات الحواف الموثقة

عبداللطيف محمد الخليفي و هومايون كبير
قسم الهندسة المدنية – جامعة الكويت
ص.ب. 5969 الصفاة – الكويت 13060
و
سان – شيان لين
قسم هندسة الموانىء والأنهار – جامعة تايوان (المحيط)
تايبي – تايوان

خلاصة

يتم تحليل صفيحة أسطوانية ذات حواف موثقة من مادة متجانسة باستخدام طريقة تم تطويرها حديثاً كما تستخدم طريقة العنصر المحدود لمعايرة الطريقة المطورة هنا ويستخدم التحليل طريقة متوالية فوريير المزدوجة لحالات السماكة المعتدلة كما أن طريقة العنصر المحدود مبينة على عنصر ذو أربعة عقد كالذي في برنامج STAAD-III ويكون تكوين القشرة للعمق الكلي للطريقتين بناء على نظرية القص التشوهي من الدرجة الأولى أما النتائج التحليلية المستنبطة والمقارنات المقدمة لتأثيرات عدة عوامل فإنها تعتبر بمثابة خطوط استدلال للمهندسين.